Courbure discrète : théorie et applications

Rencontre organisée par :
Laurent Najman and Pascal Romon

18-22 novembre 2013

Atsushi Imiya

Curvature and Flow in Digital Space

Vol. 3, n° 1 (2013), p. 183-194.

<http://acirm.cedram.org/item?id=ACIRM_2013__3_1_183_0>

Centre international de rencontres mathématiques
U.M.S. 822 C.N.R.S./S.M.F.
Luminy (Marseille) France

Actes des rencontres du C.I.R.M.
Vol. **3** n° 1 (2013) 183-194

Curvature and Flow in Digital Space

Atsushi Imiya

Abstract

We first define the curvature indices of vertices of digital objects. Second, using these indices, we define the principal normal vectors of digital curves and surfaces. These definitions allow us to derive the Gauss-Bonnet theorem for digital objects. Third, we introduce curvature flow for isothetic polytopes defined in a digital space.

1. Introduction

A unified treatment of shape deformation is required for the intelligent editing of image contents for multimedia technology. The deformation of image data based on curvature flow and diffusion processes [17, 18, 29, 21] on surfaces [13, 22] provides a mathematical foundation for the unified treatment of deformation [23].

These deformation operations for boundaries are discussed in the framework of the free boundary problem in mathematics. For the construction of solutions of partial differential equations as deformed surfaces, the numerical computation is achieved using an appropriate discretization scheme [13, 1]. Bruckstein *et al.* derived a digital version of this problem for planar shapes [7]. Furthermore, Bobenko and Suris proposed a spatial version of their digital treatment [6].

In this paper, we introduce a transform [12] for a binary digital set [14], which we call *Digital Curvature Flow*. Digital curvature flow describes the geometric flow [7, 10] controlled by the curvature on the boundary of binary digital images on a plane and in a space. This flow, which moves the boundary, can also be considered as the curvature flow on isothetic polytopes of which all edges are parallel to axes of the orthogonal coordinate system [14].

For the numerical analysis of partial differential equations, it is required to generate grids [28] or decompose the region of interest to small domains [27] for the discretization of equations [19, 9, 20]. Therefore, numerical analysis is achieved in discrete forms. However, these grids usually depend on problems which we want to deal with. In contrast to this classical numerical treatment [27, 28], in this paper, we define the digital treatment of the deformation of the boundary of an object in a digital space which is defined as a collection of lattice points [14].

Control of the topology is an important problem for flow-based shape analysis and processing [13, 22, 7]. Curvature flows usually cause the collapse of the topology. Therefore, we propose a method for the examination of the topology of digital shapes and objects. Using this process we can detect collapses of topologies and control the topology of shapes and objects during deformation by flow-based processing.

Since the curvature of a point on curves and surfaces is defined locally [26, 24, 31, 25], the curvature flow is basically a local operation on them. As a digital treatment of partial differential equations, the theory of cellular automaton is proposed. In this theory, a space is also digitized and equations are approximately expressed as rules which rewrite the configurations of 1-points in a neighbourhood of a digital space [15, 14]. Therefore, rules for the cellular-automaton treatment [16, 8, 30] of partial differential equations are basically local operations. These similar properties

Text presented during the meeting "Discrete curvature: Theory and applications" organized by Laurent Najman and Pascal Romon. 18-22 novembre 2013, C.I.R.M. (Luminy).
2000 *Mathematics Subject Classification.* 52C07,65Q10,68R10.
Key words. Digital Space, Surgery, Curvature flow, Topology.

between cellular automata and curvature suggest that our treatment of boundary deformation is natural from the viewpoint of space discretization.

2. Connectivity and Neighbourhood

Setting $\mathbf{R}^2$ and $\mathbf{R}^3$ to be two- and three-dimensional Euclidean spaces, we express vectors in $\mathbf{R}^2$ and $\mathbf{R}^3$ as $\boldsymbol{x} = (x, y)^\top$ and $\boldsymbol{x} = (x, y, z)^\top$, respectively, where $\top$ is the transpose of the vector. Setting $\mathbf{Z}$ to be the set of all integers, the two- and three-dimensional digital spaces $\mathbf{Z}^2$ and $\mathbf{Z}^3$ are sets of points such that both x and y are integers and x, y and z are all integers, respectively.

On $\mathbf{Z}^2$ and in $\mathbf{Z}^3$

$$\mathbf{N}^4((m,n)^\top) = \{(m \pm 1, n)^\top, (m, n \pm 1)^\top\} \tag{2.1}$$

and

$$\mathbf{N}^6((k,m,n)^\top) = \{(k \pm 1, m, n)^\top, (k, m \pm 1, n)^\top, (k, m, n \pm 1)^\top\}$$

are the planar 4-neighbourhood of point $(m, n)^\top$ and the spatial 6-neighbourhood of point $(k, m, n)^\top$, respectively. In this paper, we assume 4-connectivity on $\mathbf{Z}^2$ and 6-connectivity in $\mathbf{Z}^3$.

For integers k, m and n, the collection of integer triplets (k', m', n') which satisfy the equation

$$(k - k')^2 + (m - m')^2 + (n - n')^2 = 1 \tag{2.2}$$

defines points in the 6-neighbourhood of point $(k, m, n)^\top$. If we substitute $k = k'$, $m = m'$ and $n = n'$ into eq. (2.2), we obtain the equations

$$(m - m')^2 + (n - n')^2 = 1, \;\; (k - k')^2 + (n - n')^2 = 1, \;\; (m - m')^2 + (n - n')^2 = 1. \tag{2.3}$$

These equations define points in the planar 4-neighbourhoods. Therefore, setting one of x, y or z to be a fixed integer, we obtain two-dimensional sets of lattice points such that

$$\mathbf{Z}_1^2((k,m,n)^\top) = \{(k,m,n)^\top | \exists k, \forall m, \forall n \in \mathbf{Z}\}, \tag{2.4}$$

$$\mathbf{Z}_2^2((k,m,n)^\top) = \{(k,m,n)^\top | \forall k, \exists m, \forall n \in \mathbf{Z}\}, \tag{2.5}$$

and

$$\mathbf{Z}_3^2((k,m,n)^\top) = \{(k,m,n)^\top | \forall k, \forall m, \exists n \in \mathbf{Z}\}. \tag{2.6}$$

These two-dimensional digital spaces are mutually orthogonal. Denoting

$$\mathbf{N}_1^4((k,m,n)^\top) = \{(k, m \pm 1, n)^\top, (k, m, n \pm 1)^\top\}, \tag{2.7}$$

$$\mathbf{N}_2^4((k,m,n)^\top) = \{(k \pm 1, m, n)^\top, (k, m, n \pm 1)^\top\}, \tag{2.8}$$

and

$$\mathbf{N}_3^4((k,m,n)^\top) = \{(k \pm 1, m, n)^\top, (k, m \pm 1, n)^\top\}, \tag{2.9}$$

the relationship

$$\mathbf{N}^6((k,m,n)^\top) = \mathbf{N}_1^4((k,m,n)^\top) \cup \mathbf{N}_2^4((k,m,n)^\top) \cup \mathbf{N}_3^4((k,m,n)^\top)$$

holds since $\mathbf{N}_i^4((k,m,n)^\top)$ is the 4-neighbourhood on the plane $\mathbf{Z}_i^2((k,m,n)^\top)$ for $i = 1, 2, 3$ [11]. Equation (2.10) implies that the 6-neighbourhood is decomposed into three mutually orthogonal 4-neighbourhoods [11]. Figures 2.1 (a) and (b) illustrate the spatial 6-neighbourhood and planar 4-neighbourhood, respectively. The 6-neighbourfood in $\mathbf{Z}^3$ is decomposed into three mutually orthogonal 4-neighbourhoods as shown in Figure 2.1 (c).

A pair of points $(k, m, n)^\top$ and $\boldsymbol{x} \in \mathbf{N}^6((k,m,n)^\top)$ defines a unit line segment in $\mathbf{Z}^3$. Furthermore, four 6-connected points which form a circle define a unit plane segment in $\mathbf{Z}^3$ with respect to the 6-connectivity. Therefore, we assume that our object is a complex of $2 \times 2 \times 2$ cubes which share at least one face with each other. Thus, the surface of an object is a collection of unit squares which are parallel to the planes $x = 0$, $y = 0$ and $z = 0$.

Definition 1. For a point $\boldsymbol{x} \in \mathbf{Z}^3$, the collection of eight points

$$S^3 = \{\boldsymbol{x}, \boldsymbol{x} + \boldsymbol{e}_1, \boldsymbol{x} + \boldsymbol{e}_2, \boldsymbol{x} + \boldsymbol{e}_3, \boldsymbol{x} + \boldsymbol{e}_1 + \boldsymbol{e}_2, \boldsymbol{x} + \boldsymbol{e}_2 + \boldsymbol{e}_3, \boldsymbol{x} + \boldsymbol{e}_3 + \boldsymbol{e}_1, \boldsymbol{x} + \boldsymbol{e}_1 + \boldsymbol{e}_2 + \boldsymbol{e}_2\} \tag{2.10}$$

is a digital 3-simplex.

Definition 2. A digital object is a complex of a finite number of digital 3-simplices.

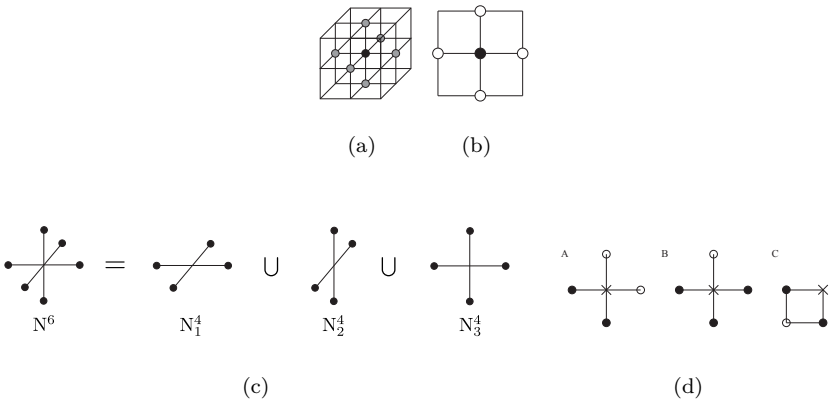

Figure 2.1: Local configuration of 2-manifold in $\mathbf{Z}^3$. (a) 6-neighbourhood in $\mathbf{Z}^3$ (b) 4-neighbourhood on $\mathbf{Z}^2$. (c) Decomposition of the 6-neighbourhood in the space to 4-neighbourhoods on the three orthogonal planes. (d) Configurations of points on the planar boundary. The spatial 6-neighbourfood in $\mathbf{Z}^3$ is decomposed into three mutually orthogonal 4-neighbourhoods.

3. Digital Boundary Manifold

For a pair of sets $\boldsymbol{A}$ and $\boldsymbol{B}$ in $\mathbf{R}^n$, the Minkowski addition $\boldsymbol{A} \oplus \boldsymbol{B}$ and the Minkowski subtraction $\boldsymbol{A} \ominus \boldsymbol{B}$ are defined as

$$\boldsymbol{A} \oplus \boldsymbol{B} = \bigcup_{\boldsymbol{b} \in \boldsymbol{B}} \boldsymbol{A}(\boldsymbol{b}), \ \boldsymbol{A} \ominus \boldsymbol{B} = \bigcap_{\boldsymbol{b} \in \boldsymbol{B}} \boldsymbol{A}(\boldsymbol{b}), \tag{3.1}$$

for $\boldsymbol{A}(\boldsymbol{x}) = \{\boldsymbol{y} | \boldsymbol{y} = \boldsymbol{a} + \boldsymbol{x}, \forall \boldsymbol{a} \in \boldsymbol{A}\}$.

For the Minkowski addition and subtraction, the relations

$$\boldsymbol{F} \ominus \boldsymbol{G} = \overline{\boldsymbol{F} \oplus \overline{\boldsymbol{G}}} \tag{3.2}$$

$$\boldsymbol{F} \oplus (\boldsymbol{G} \cup \boldsymbol{H}) = (\boldsymbol{F} \oplus \boldsymbol{G}) \cup (\boldsymbol{F} \oplus \boldsymbol{H}) \tag{3.3}$$

$$\boldsymbol{F} \ominus (\boldsymbol{G} \cup \boldsymbol{H}) = (\boldsymbol{F} \ominus \boldsymbol{G}) \cap (\boldsymbol{F} \ominus \boldsymbol{H}) \tag{3.4}$$

are satisfied. Furthermore, we obtain the following theorem.

Theorem 3. *If $\boldsymbol{F} \cap \boldsymbol{G} = \emptyset$, the equality*

$$(\boldsymbol{F} \cup \boldsymbol{G}) \ominus \boldsymbol{H} = (\boldsymbol{F} \ominus \boldsymbol{H}) \cup (\boldsymbol{G} \ominus \boldsymbol{H}) \tag{3.5}$$

is satisfied

(*Proof*)

$$\begin{aligned}
(\boldsymbol{F} \cup \boldsymbol{G}) \ominus \boldsymbol{H} &= \bigcap_{\boldsymbol{x} \in \boldsymbol{H}} (\boldsymbol{F} \cup \boldsymbol{G})(\boldsymbol{x}) \\
&= \{\boldsymbol{x} + \boldsymbol{y} | \forall \boldsymbol{x} \in \boldsymbol{H}, \exists \boldsymbol{y} \in (\boldsymbol{F} \cup \boldsymbol{G})\} \\
&= \{\boldsymbol{x} + \boldsymbol{y} | \forall \boldsymbol{x} \in \boldsymbol{H}, \exists \boldsymbol{y} \in \boldsymbol{F}\} \cup \{\boldsymbol{x} + \boldsymbol{y} | \forall \boldsymbol{x} \in \boldsymbol{H}, \exists \boldsymbol{y} \in \boldsymbol{G}\} \\
&= (\boldsymbol{F} \ominus \boldsymbol{H}) \cup (\boldsymbol{G} \ominus \boldsymbol{H})
\end{aligned}$$

□

In $\mathbf{Z}^3$, the inner boundary of $\mathbf{F}$ is defined as

$$\partial \mathbf{F} = \mathbf{F} \setminus (\mathbf{F} \ominus \mathbf{N}^6), \tag{3.6}$$

where $\mathbf{N}^6 = \mathbf{N}^6((0,0,0)^\top)$. A polyhedron whose vertices are points in $\partial \mathbf{F}$ is a Nef polyhedron [4, 2, 3, 5]. Therefore, the inner boundary of $\mathbf{F}$ is a Nef polyhedron.

Definition 4. We call a Nef polyhedron in $\mathbf{Z}^3$ a grid Nef polyhedron.

In this paper, we deal with the topological and geometrical properties of grid points on the surface of a grid Nef polyhedron.

For $i = 1, 2, 3$, we set

$$\mathbf{Z}^2_{k(i)} = \{\boldsymbol{x} | \boldsymbol{x} = \boldsymbol{z} + k(i)\boldsymbol{e}_i, \boldsymbol{z} \in \mathbf{Z}^2_i((0,0,0)^\top)\}, \tag{3.7}$$

where $\boldsymbol{e}_1 = (1,0,0)^\top$, $\boldsymbol{e}_2 = (0,1,0)^\top$ and $\boldsymbol{e}_3 = (0,0,1)^\top$. A slice of $\mathbf{F}$ perpendicular to the plane $\mathbf{Z}^2_i$ for $i = 1, 2, 3$ is

$$\mathbf{F}^2_{k(i)} = \mathbf{F} \cap \mathbf{Z}^2_{k(i)}, \tag{3.8}$$

Furthermore, we set

$$K(i) = \{k(i) | \mathbf{F} \cap \mathbf{Z}^2_{k(i)} \neq \emptyset\}, \tag{3.9}$$

that is, $K(i)$ is the number of slices which are perpendicular to $\boldsymbol{e}_i$. We have the following decomposition theorem.

Theorem 5. *Setting*

$$\partial\mathbf{F}^2_{k(i)} = \mathbf{F}^2_{k(i)} \setminus (\mathbf{F}^2_{k(i)} \ominus \mathbf{N}^4_i), \tag{3.10}$$

where $\mathbf{N}^4_i = \mathbf{N}((0,0,0)^\top)$*, the relation*

$$\partial\mathbf{F} = \bigcup_{i=1}^{3} \bigcup_{k(i)\in K(i)} \partial\mathbf{F}^2_{k(i)} \tag{3.11}$$

is satisfied.

(*Proof*) Since $\mathbf{N}^6 = \bigcup_{i=1}^3 \mathbf{N}^4_i$, we have the relation $\mathbf{F} \ominus \mathbf{N}^6 = \bigcup_{i=1}^3 (\mathbf{F} \ominus \mathbf{N}^4_i)$. Furthermore, the decomposition $\mathbf{F} = \bigcup_{i=1}^3 \left\{ \bigcup_{k(i)\in K(i)} \mathbf{F}^2_{k(i)} \right\}$ derives the relation

$$\begin{aligned} \mathbf{F} \setminus (\mathbf{F} \ominus \mathbf{N}^6) &= \left(\bigcup_{i=1}^{3} \bigcup_{k(i)\in K(i)} \mathbf{F}^2_{k(i)} \right) \setminus \left\{ \bigcup_{i=1}^{3} ((\bigcup_{k(i)\in K(i)} \mathbf{F}^2_{k(i)}) \ominus \mathbf{N}^4_i) \right\} \\ &= \bigcup_{i=1}^{3} \bigcup_{k(i)\in K(i)} \left\{ \mathbf{F}^2_{k(i)} \setminus (\mathbf{F}^2_{k(i)} \ominus \mathbf{N}^4_i) \right\}. \end{aligned} \tag{3.12}$$

□

Theorem 5 implies the following properties.

Property 6. *On the surface of a grid Nef polyhedron, each point lies on two or three digital planes.*

Property 7. *The boundary* $\partial\mathbf{F}$ *of a three-dimensional digital object* $\mathbf{F}$ *is the union of the two-dimensional boundaries.*

Therefore, it is possible to construct $\partial\mathbf{F}$ from $\{\partial\mathbf{F}^2_{k(i)}\}^3_{k(i)\in K(i),i=1}$. Using this relation recursively, we can construct the boundary detection algorithm for three-dimensional digital objects from two-dimensional boundary detection algorithms.

4. Curvature Indices of Points

4.1. **Planar Curvature Indices.** Since we are concerned with a binary digital object, we affix values of 0 and 1 to points in the background and in objects, respectively. On $\mathbf{Z}^2$, the three types of point configurations illustrated in Figure 2.1 (d) exist in the neighbourhood of a point $\times$ on the boundary. In the three configurations A, B and C in Figure 2.1 (d), $\bullet$ and $\circ$ are points on the boundary and in the background, respectively. Setting $f_i \in \{0, 1\}$ to be the value of point $\boldsymbol{x}_i$ such that

$$\begin{array}{ccc} & \boldsymbol{x}_3 = (m, n+1)^\top & \\ \boldsymbol{x}_5 = (m-1, n)^\top & \boldsymbol{x}_0 = (m, n)^\top & \boldsymbol{x}_1 = (m+1, n)^\top \\ & \boldsymbol{x}_7 = (m, n-1)^\top, & \end{array} \tag{4.1}$$

the curvature of point $\boldsymbol{x}_0$ is defined by

$$r(\boldsymbol{x}_0) = 1 - \frac{1}{2}\sum_{k\in N} f_k + \frac{1}{4}\sum_{k\in N} f_k f_{k+1} f_{k+2}, \tag{4.2}$$

where $N = \{1, 3, 5, 7\}$ and $k + 8 = k$ [24]. The curvature indices of configurations (a), (b) and (c) are positive, zero and negative, respectively. Therefore, we call these configurations convex, flat and concave, and affix the indices $+$, 0 and $-$, respectively.

4.2. **Spatial Curvature Indices.** Using combinations of planar curvature indices on three mutually orthogonal planes passing through a point $\boldsymbol{x}_0$, we define the curvature index of a point $\boldsymbol{x}_0$ in $\mathbf{Z}^3$ since the 6-neighbourhood is decomposed into three 4-neighbourhoods. On the boundary of a 6-connected object, Theorem 5 implies that there exist nine configurations in the $3 \times 3 \times 3$ local neighbourhoods shown in Figure 4.1.

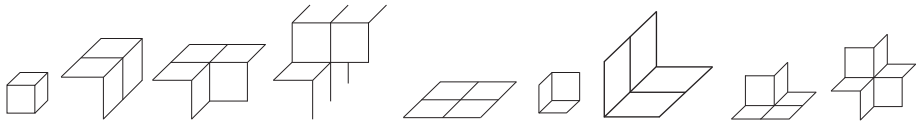

Figure 4.1: Local configurations of 2-manifold in $\mathbf{Z}^3$

Setting α_i to be the planar curvature index on plane $\mathbf{Z}_i^2(k(i))$ for $i = 1, 2, 3$, the curvature index of a point in $\mathbf{Z}^3$ is a triplet of two-dimensional curvature indices $(\alpha_1, \alpha_2, \alpha_3)$ such that $\alpha_i \in \{+, -, 0, \emptyset\}$. Here, if $\alpha_i = \emptyset$, the curvature index of a point on the plane $\mathbf{Z}_i^2(k(i))$ is not defined. Therefore, for the boundary points, seven configurations,

$$\begin{array}{ccc} (+,+,+), & (+,+,-), & (+,0,0), \\ & (0,0,\emptyset), & \\ (-,-,-), & (+,-,-), & (-,0,0), \end{array} \tag{4.3}$$

and their permutations are possible [11]. For a spatial curvature index α, setting $n(\alpha)$ to be the number of octspaces in the $3 \times 3 \times 3$ neighbourhood of a point, we have the relations

$$\begin{array}{lll} n((+,+,+)) = 1, & n((+,+,-)) = 3, & n((+,0,0)) = 2, \\ & n((0,0,\emptyset)) = 4, & \\ n((-,-,-)) = 4,7, & n((+,-,-)) = 4,5, & n((-,0,0)) = 6. \end{array} \tag{4.4}$$

Since there exist two configurations for $(-,-,-)$ and $(+,-,-)$, we set

$$n((-,-,-)) = 7,\ n((-,-,-)_-) = 4,\ n((+,-,-)) = 5,\ n((+,-,-)_+) = 4. \tag{4.5}$$

Furthermore, since $\frac{i}{8} = 1 - \frac{8-i}{8}$, the vertex angles of the nine configurations on the boundary are

$$\begin{array}{lll} \gamma((+,+,+)) = \frac{1}{8}, & \gamma((+,0,0)) = \frac{2}{8}, & \gamma((+,+,-)) = \frac{3}{8}, \\ \gamma((+,-,-)_+) = \frac{4}{8}, & \gamma((0,0,\emptyset)) = 0, & \gamma((-,-,-)_-) = \frac{-4}{8}, \\ \gamma((+,-,-)) = \frac{-3}{8}, & \gamma(-,0,0) = \frac{-2}{8}, & \gamma((-,-,-)) = \frac{-1}{8}. \end{array} \tag{4.6}$$

Definition 8. Using the nine configurations of eq. (4.6), we define the relation between the codes and the triplet vectors $\boldsymbol{\alpha}(\boldsymbol{x})$ for point $\boldsymbol{x}$ as

$$
\begin{array}{llll}
\boldsymbol{\alpha}(\boldsymbol{x}) & \gamma(\boldsymbol{x}) & \boldsymbol{\alpha}(\boldsymbol{x}) & \gamma(\boldsymbol{x}) \\
(1,1,1)^\top & (0,0,+) & (1,1,-1)^\top & (+,+,-) \\
 & (0,+,0) & & (-,-,+) \\
 & (+,0,0) & (1,-1,1)^\top & (+,-,+) \\
 & (+,+,+) & & (-,+,-) \\
 & (-,-,-) & (-1,1,1)^\top & (-,+,+) \\
 & (0,0,-) & & (+,-,-) \\
 & (0,-,0) & (1,1,0)^\top & (0,0,\emptyset) \\
 & (-,0,0) & (1,0,1)^\top & (0,\emptyset,0) \\
 & & (0,1,1)^\top & (\emptyset,0,0).
\end{array}
\tag{4.7}
$$

Definition 9. Setting $s(\pm) = \pm 1$, $s(0) = 0$ and $s(\emptyset) = 0$, we define the vertex indices as

$$
f(\alpha_1,\alpha_2,\alpha_3) = (s(\alpha_1)+s(\alpha_2)+s(\alpha_3)) \times (|s(\alpha_1)| + |s(\alpha_2)+|s(\alpha_3)|)
\tag{4.8}
$$

using eq. (4.7).

This function $f(\cdot,\cdot,\cdot)$ takes values of $\{0,\pm 1,\pm 3,\pm 9\}$ according to the configurations on the boundary. Furthermore, the sign of the function $f(\alpha_1,\alpha_2,\alpha_3)$ indicates the direction of normal vector $\boldsymbol{n}(\boldsymbol{x})$ at point $\boldsymbol{x}$ on the boundary. The direction of the normal vector is outward or inward if the sign is positive or negative, respectively.

Setting n_i to be the number of points whose vertex angles are $\frac{i}{8}$, we define three vectors,

$$
\boldsymbol{n} = (n_{-4},n_{-3},n_{-2},n_{-1},n_0,n_1,n_2,n_3,n_4)^\top
\tag{4.9}
$$

$$
\boldsymbol{a} = (-2,-1,0,1,0,1,0,-1,-2)^\top,
\tag{4.10}
$$

$$
\boldsymbol{k} = \boldsymbol{a}^2 = (4,1,0,1,0,1,0,1,4)^\top.
\tag{4.11}
$$

Using these vectors, we have the following theorems for the Euler characteristics of digital objects [4, 2, 3, 5].

Theorem 10. *An object* $\mathbf{F}$ *without tunnels satisfies the relationship*

$$
\boldsymbol{a}^\top \boldsymbol{n} = 8.
\tag{4.12}
$$

Theorem 11. *A collection of objects* $\{\mathbf{F}_i\}_{i=1}^n$*, with* g_i *tunnels satisfies the relationship*

$$
\boldsymbol{a}^\top \boldsymbol{n} = 8\sum_{i=1}^{n}(1-g_i).
\tag{4.13}
$$

5. Digital Curvature Flow

5.1. **Normal Vectors on Digital Plane.** For $n = 2, 3$ we define the dual set for the set lattice points $\mathbf{Z}^n$ as

$$
\overline{\mathbf{Z}^n} = \{\boldsymbol{x} + \frac{1}{2}\boldsymbol{e} | \boldsymbol{x} \in \mathbf{Z}^n\},
\tag{5.1}
$$

where $\boldsymbol{e} = (1,1)^\top$ and $\boldsymbol{e} = (1,1,1)^\top$ for $n = 2$ and $n = 3$, respectively. We call $\mathbf{Z}^n$ and $\overline{\mathbf{Z}^n}$ the lattice and the dual lattice, respectively. Using the lattice and the dual lattice, we define the curvature flow for surfaces defined in the lattice space.

We first deal with a closed planar curve. Setting $\mathbf{C} = \{\boldsymbol{x}_j\}_{j=1}^N$ to be the set of points on the boundary $\partial\mathbf{F}_{k(i)}$ for fixed i and $K(i)$, we assume that only two points $\boldsymbol{x}_{j=1}$ and $\boldsymbol{x}_{j+1}$ are connected for each i and that the triplet $\boldsymbol{x}_{j-1}$, $\boldsymbol{x}_j$ and $\boldsymbol{x}_{j+1}$ lies in the anticlockwise direction on the boundary.

Using triplet of points $\boldsymbol{x}_{j-1}$, $\boldsymbol{x}_j$ and $\boldsymbol{x}_{j+1}$, we compute the normal vector of each point. For the planar point $\boldsymbol{x}_j = (x_j, y_j)^\top$, we express this vector as the complex number $z_j = x_j + iy_j$. Setting

$$
\alpha_j + i\beta_j = \left(\frac{z_{j+1}-z_j}{z_{j-1}-z_j}\right)^{\frac{1}{2}},
\tag{5.2}
$$

we define the outward normal vector $\boldsymbol{n}_j$ as

$$\boldsymbol{n}_j = \lambda \boldsymbol{a}_j,\ \boldsymbol{a}_j = (\alpha_j, \beta_j)^\top, \tag{5.3}$$

for point $\boldsymbol{x}_j$. From the local configurations of triplets of vectors on the boundary, there exist three combinations for α_j and β_j:

(1) $|\alpha_j| = 1/\sqrt{2}$ and $|\beta_j| = 1/\sqrt{2}$,
(2) $|\alpha_j| = 0$ and $|\beta_j| \neq 0$,
(3) $|\alpha_j| \neq 0$ and $|\beta_j| = 0$.

These geometrical relations imply that

$$\lambda_j = \begin{cases} \frac{1}{2} & \text{if } \alpha_j \beta_j = 0, \\ \frac{1}{\sqrt{2}} & \text{otherwise.} \end{cases} \tag{5.4}$$

Figure 5.1 shows the directions of normal vectors on a digital curve on a plane.

Figure 5.1: Normal vectors on the corner. On the digital boundary, there exist three configurations of the normal vectors of the point.

Using the curvature code $\gamma(\boldsymbol{x}_j)$ of each point $\boldsymbol{x}_j$, we classify points on the boundary $\mathbf{C} := \partial \mathbf{F}_{k(i)}$ for fixed i and $k(i)$ into types $\mathbf{N}_+$ and $\mathbf{N}_-$.

Definition 12. For a sequence of flat points

$$\mathbf{N}_-(j) = \{\boldsymbol{x}_\beta | \gamma(\boldsymbol{x}_\beta) = 0,\ j < \beta < j + m,\ s(\gamma(\boldsymbol{x}_j)) \times s(\gamma(\boldsymbol{x}_{j+m})) = -1\}, \tag{5.5}$$

where $s(\gamma(\boldsymbol{x})) = 1$ and $s(\gamma(\boldsymbol{x})) = -1$ for $(\gamma(\boldsymbol{x}_j) and \gamma(\boldsymbol{x}_{j+m})) = (+, -)$ and $(\gamma(\boldsymbol{x}_j) and \gamma(\boldsymbol{x}_{j+m})) = (-, +)$, respectively.

Each $\mathbf{N}_-(j)$ is a sequence of flat points whose one endpoint is the concave point. Then, we set

$$\mathbf{N}_- = \bigcup_j \mathbf{N}_-(j),\ \mathbf{N}_+ = \mathbf{C} \setminus \mathbf{N}_-. \tag{5.6}$$

Since $\mathbf{N}_-$ is the union of sequences whose one endpoint is the concave point on the boundary, we have the relation

$$\mathbf{C} = \mathbf{N}_+ \bigcup \mathbf{N}_-,\ \mathbf{N}_+ \bigcap \mathbf{N}_- = \emptyset. \tag{5.7}$$

Therefore, points in $\mathbf{N}_+$ and $\mathbf{N}_-$ lie in convex and concave parts on the original boundary, respectively.

Definition 13. If an end of a line segment is negative, we say that this line segment is a negative line segment. Furthermore, if both ends are positive, we say that this line segment is a positive line segment.

Using these geometrical properties of point sets $\mathbf{N}_+$ and $\mathbf{N}_-$ on the boundary, we define a global transform from point set $\mathbf{C}$ on $\mathbf{Z}^2$ to point set $\overline{\mathbf{C}}$ on $\overline{\mathbf{Z}^2}$ as

$$\overline{\boldsymbol{x}}_j = \begin{cases} \boldsymbol{x}_j - \boldsymbol{n}_j, & \text{if } \gamma(\boldsymbol{x}_j) \neq 0, \\ \boldsymbol{x}_j - \boldsymbol{n}_j \pm \frac{1}{2}\boldsymbol{n}_j^\top, & \text{if } \gamma(\boldsymbol{x}_j) = 0,\ \boldsymbol{x}_j \in \mathbf{N}_+, \\ \boldsymbol{x}_j + \boldsymbol{n}_j \pm \frac{1}{2}\boldsymbol{n}_j^\top, & \text{if } \gamma(\boldsymbol{x}_j) = 0,\ \boldsymbol{x}_j \in \mathbf{N}_-. \end{cases} \tag{5.8}$$

5.2. **Normal Vectors in Digital Space.** Point configurations on the boundary are defined by the digital lines which lie on two or three mutually orthogonal vectors. Therefore, we define three normal vectors $\boldsymbol{n}_1$, $\boldsymbol{n}_2$ and $\boldsymbol{n}_3$ which lie on planes perpendicular to vectors $\boldsymbol{e}_1$, $\boldsymbol{e}_2$ and $\boldsymbol{e}_3$, respectively. According to these definitions, for $\boldsymbol{n} = (\alpha, \beta)^\top$ on each plane, we have

$$\boldsymbol{n}_1 = (0, \alpha, \beta)^\top,\ \boldsymbol{n}_2 = (\alpha, 0, \beta)^\top,\ \boldsymbol{n}_3 = (\alpha, \beta, 0)^\top. \tag{5.9}$$

Using the vector $\boldsymbol{n}_\alpha$, $\alpha = 1, 2, 3$, we define the normal vector $\boldsymbol{n}(\boldsymbol{x})$ for a point $\boldsymbol{x}$ on the boundary $\mathbf{S}$ in digital space $\mathbf{Z}^3$. There are nine types of vertex configurations in a $3 \times 3 \times 3$ neighbourhood on the boundary. Using eq. (4.7), we define the normal vector $\boldsymbol{n}(\boldsymbol{x})$ of point $\boldsymbol{x}$.

Definition 14. The normal vector of a point $\boldsymbol{x} \in \mathbf{Z}^3$ is

$$\boldsymbol{n}(\boldsymbol{x}) = \frac{1}{2}\boldsymbol{N}\boldsymbol{\alpha}(\boldsymbol{x}) \tag{5.10}$$

for matrix $\boldsymbol{N} = (\boldsymbol{n}_1, \boldsymbol{n}_2, \boldsymbol{n}_3)$ on the surface of a Nef polyhedron.

5.3. **Curvature-based Motion of Points.** We derive a transformation using the global information of the concavity of the digital boundary.

Definition 15. For boundary points whose two-dimensional codes are zero, we affix the same two-dimensional curvature codes with these of line segments on which points lie.

The rule of Definition 15 derives the codes $(\alpha, \beta_1, \beta_2)$, $(\beta_1, \alpha, \beta_2)$ and $(\beta_1, \beta_2, \alpha)$, where $\beta_i \in \{+, -\}$, for a point whose codes are $(\alpha, 0, 0)$, $(0, \alpha, 0)$ and $(0, 0, \alpha)$, where $\alpha \in \{+, -, \emptyset\}$. These notations lead to the codes $(+, +, +)$, $(+, +, -)$, $(+, -, -)$, $(-, -, -)$, $(\emptyset, +, +)$, $(\emptyset, +, -)$, $(\emptyset, -, -)$ and their permutations. Using these codes, we define the code of the flat points and points on edges as

$$g(\alpha, \beta_1, \beta_2) = \begin{cases} +, & \text{if } f(\alpha, \beta_1, \beta_2) = 9, \\ -, & \text{otherwise,} \end{cases} \tag{5.11}$$

for $(\alpha, \beta_1, \beta_2)$ and its permutations.

Setting

$$h(\beta_1, \beta_2) = (s(\beta_1) + s(\beta_2)) \times (|s(\beta_1)| + |s(\beta_2)|), \tag{5.12}$$

we set the codes of flat points and points on edges as positive and negative if $h(\beta_1, \beta_2) > 0$ and otherwise, respectively. For these curvature codes, the code of a flat point is defined as negative if the number of negative codes in the curvature code is positive. Furthermore, we move flat points outward and inward, if the codes are positive and negative, respectively.

Definition 16. For two line segments, which are mutually orthogonal, pass through flat points with codes $(\emptyset, 0, 0)$, $(0, \emptyset, 0)$ and $(0, 0, \emptyset)$, using the codes of the end points of these two line segments on a plane, we can affix the codes of flat points. Furthermore, If at least one end point is negative, we assign the negative code to a point on this line.

There are six possibilities for the configurations of end points of two mutually orthogonal line segments. These definitions for codes also conclude that the codes of points with the curvature codes $(+, 0, 0)$, $(0, +, 0)$ and $(0, 0, +)$ on an edge are negative if one end or both ends are negative. Figure 5.2 shows examples of the signs of vertex indices on the boundary.

The normal vector on the discrete surface defined by eq. (5.10) is in the form

$$\boldsymbol{n}(\boldsymbol{x}) = \frac{1}{2}(a_1\boldsymbol{e}_1 + a_2\boldsymbol{e}_2 + a_3\boldsymbol{e}_3), \tag{5.13}$$

where $a_i \in \{-1, 0, 1\}$. Therefore, if $a_i = 1$ and $a_i = -1$, the vector $(\boldsymbol{x} + \boldsymbol{n}(\boldsymbol{x}))$ determines the transformation from $\boldsymbol{x} \in \mathbf{Z}^3$ to $\boldsymbol{y} \in \overline{\mathbf{Z}^3}$. Moreover, if and only if the codes are $(+, +, +)$, $(-, -, -)$, and $(-, -, -)_-$ and (α, β, γ) for $\alpha, \beta, \gamma \in \{+, -\}$, the vector $(\boldsymbol{x} + \boldsymbol{n}(\boldsymbol{x}))$ determines the transformation from $\boldsymbol{x} \in \mathbf{Z}^3$ to $\boldsymbol{y} \in \overline{\mathbf{Z}^3}$.

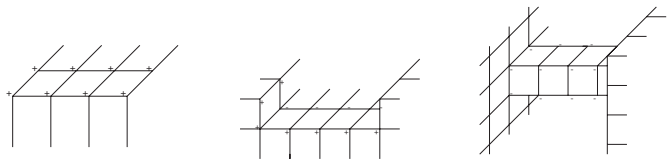

(a) (b) (c)

Figure 5.2: Signs for flat points and edges.

For the codes $(-,-,-)$, $(\alpha,0,0)$, $(\alpha,0,0)$ and $(0,0,\alpha)$ for $\alpha \in \{+,-,\emptyset\}$, the normal vectors hold the relations

$$
\begin{array}{llllll}
\alpha(\boldsymbol{x}) & (\emptyset,0,0) & (0,\emptyset,0) & (0,0,\emptyset) & (-,-,-) \\
\boldsymbol{n}(\boldsymbol{x}) & \mathbf{0} & \mathbf{0} & \mathbf{0} & a_i\boldsymbol{e}_i + a_j\boldsymbol{e}_j \\
\alpha(\boldsymbol{x}) & (\pm,0,0) & (0,\pm,0) & (0,0,\pm) & \\
\boldsymbol{n}(\boldsymbol{x}) & \pm\frac{1}{2}(a_2\boldsymbol{e}_2 + a_3\boldsymbol{e}_3) & \pm\frac{1}{2}(a_1\boldsymbol{e}_1 + a_3\boldsymbol{e}_3) & \pm\frac{1}{2}(a_1\boldsymbol{e}_1 + a_2\boldsymbol{e}_2). &
\end{array}
\tag{5.14}
$$

However, these normal vectors do not define the transformation from points in $\mathbf{Z}^3$ to $\overline{\mathbf{Z}^3}$. Therefore, we define the transformation from $\boldsymbol{x} \in \mathbf{Z}^3$ to $\boldsymbol{y} \in \overline{\mathbf{Z}^3}$ using $g(\cdot,\cdot,\cdot)$.

Definition 17. The point transformation $S(\cdot)$ between $\boldsymbol{x} \in \mathbf{Z}^3$ and $\boldsymbol{y} \in \mathbf{Z}^3$ is defined as

$$
\boldsymbol{y} = S(\boldsymbol{x}) = \boldsymbol{x} + \epsilon\boldsymbol{m}(\boldsymbol{x}) \tag{5.15}
$$

for

$$
\begin{array}{llllll}
\alpha(\boldsymbol{x}) & (\emptyset,0,0) & (0,\emptyset,0) & (0,0,\emptyset) & (-,-,-)_+ \\
\boldsymbol{m}(\boldsymbol{x}) & \pm\frac{1}{2}\boldsymbol{e}_1 & \boldsymbol{n}(\boldsymbol{x}) \pm \frac{1}{2}\boldsymbol{e}_2 & \boldsymbol{n}(\boldsymbol{x}) \pm \frac{1}{2}\boldsymbol{e}_3 & \frac{1}{2}\boldsymbol{n}(\boldsymbol{x}) \pm \frac{1}{2}\boldsymbol{e}_k \\
\alpha(\boldsymbol{x}) & (\pm,0,0) & (0,\pm,0) & (0,0,\pm) & \\
\boldsymbol{m}(\boldsymbol{x}) & \pm\frac{1}{2}(a_2\boldsymbol{e}_2 + a_3\boldsymbol{e}_3) & \pm\frac{1}{2}(a_1\boldsymbol{e}_1 + a_3\boldsymbol{e}_3) & \pm\frac{1}{2}(a_1\boldsymbol{e}_1 + a_2\boldsymbol{e}_2), &
\end{array}
\tag{5.16}
$$

where

$$
\epsilon = \begin{cases} 1, & \text{for } (+,+,+),\ (-,-,-),\ (-,-,-)_-,\ (+,+,-),\ (+,-,+) \text{ and } (-,+,+), \\ -1, & \text{for points where } g(\alpha,\beta_1,\beta_2) < 0. \end{cases} \tag{5.17}
$$

The negative sign of ϵ depends on the configuration of two mutually orthogonal line segments which pass through the points. Since the saddle points on a discrete dumbbell move inward, our method preserves the topology of the dumbbell. However, according to the definitions of the directions of the motion of points in the curvature flow, positive points on edges with both end points negative move outward. This configuration defines the outward motion for points on the bar of a dumbbell. Therefore, these definitions of the codes of flat points and edges preserve the topology of dumbbells. The successive application of eq. (5.15) defines a transformation of point sets between the lattice and the dual lattice.

Definition 18. The digital curvature flow is a sequence of point sets $\mathbf{S}_m$ for $m \geq 0$ such that

$$
\mathbf{S}_m = \begin{cases} \partial\mathbf{F} \subset \mathbf{Z}^3 & \text{if } m = 0, \\ \{\boldsymbol{x} | \boldsymbol{x} = S(\overline{\boldsymbol{x}}), \overline{\boldsymbol{x}} \in \overline{\mathbf{Z}^3}\} \subset \mathbf{Z}^3 & \text{if } m = 2k \text{ for } k \geq 1, \\ \{\overline{\boldsymbol{x}} | \overline{\boldsymbol{x}} = S(\boldsymbol{x}), \boldsymbol{x} \in \mathbf{Z}^3\} \subset \overline{\mathbf{Z}^3} & \text{otherwise.} \end{cases} \tag{5.18}
$$

The odd and even steps of the digital curvature flow transform points on the lattice to points on the dual lattice and points on the dual lattice to points on the lattice, respectively.

Now, we show an example.

Example 19. Setting lattice points on a polyhedron to be

$$
\begin{aligned}
\mathbf{P}_{10} &= \left\{ \begin{array}{lll} (0,0,2)^\top, & (0,1,2)^\top, & \\ (0,0,1)^\top, & (0,1,1)^\top, & (0,2,1)^\top \\ (0,0,0)^\top, & (0,1,0)^\top, & (0,2,0)^\top \end{array} \right\}, \\
\mathbf{P}_{11} &= \left\{ \begin{array}{lll} (1,0,2)^\top, & (1,1,2)^\top, & \\ (1,0,1)^\top, & (1,1,1)^\top, & (1,2,1)^\top \\ (1,0,0)^\top, & (1,1,0)^\top, & (1,2,0)^\top \end{array} \right\} \\
\mathbf{P}_{12} &= \left\{ \begin{array}{ll} (2,0,1)^\top, & (2,1,1)^\top \\ (2,0,0)^\top, & (2,1,0)^\top \end{array} \right\},
\end{aligned}
\tag{5.19}
$$

the digital curvature flow

$$
\begin{array}{lll}
(\frac{1}{2},\frac{1}{2},\frac{1}{2})^\top & \leftarrow & (0,0,0)^\top, \\
(\frac{1}{2},\frac{3}{2},\frac{1}{2})^\top, & \leftarrow & (0,2,1)^\top, \quad (0,2,0)^\top, \\
 & & (1,2,1)^\top, \quad (1,2,0)^\top \\
(\frac{3}{2},\frac{3}{2},\frac{1}{2})^\top & \leftarrow & (1,1,0)^\top \\
(\frac{3}{2},\frac{1}{2},\frac{1}{2})^\top, & \leftarrow & (1,0,0)^\top, \quad (2,0,0)^\top, \quad (2,1,0)^\top, \\
 & & (2,1,1)^\top, \quad (2,0,1)^\top \\
(\frac{1}{2},\frac{1}{2},\frac{3}{2})^\top, & \leftarrow & (0,0,2)^\top, \quad (0,1,2)^\top, \\
 & & (1,0,2)^\top, \quad (1,1,2)^\top, \\
(\frac{1}{2},\frac{3}{2},\frac{3}{2})^\top & \leftarrow & (0,1,1)^\top, \\
(\frac{3}{2},\frac{3}{2},\frac{3}{2})^\top & \leftarrow & (1,1,1)^\top, \\
(\frac{3}{2},\frac{1}{2},\frac{3}{2})^\top & \leftarrow & (1,0,1)^\top
\end{array}
\tag{5.20}
$$

derives the cube

$$
\mathbf{P} = \left\{ \begin{array}{lll} (\frac{1}{2},\frac{1}{2},\frac{1}{2})^\top & (\frac{1}{2},\frac{3}{2},\frac{1}{2})^\top & (\frac{3}{2},\frac{3}{2},\frac{1}{2})^\top \\ (\frac{3}{2},\frac{1}{2},\frac{1}{2})^\top & (\frac{1}{2},\frac{1}{2},\frac{3}{2})^\top & (\frac{1}{2},\frac{3}{2},\frac{3}{2})^\top \\ (\frac{3}{2},\frac{3}{2},\frac{3}{2})^\top & (\frac{3}{2},\frac{1}{2},\frac{3}{2})^\top & \end{array} \right\}.
\tag{5.21}
$$

In the next step, $\mathbf{P}$ converges to the point $(1,1,1)^\top$. Figures 5.3 (a) and (b)respectively show the original polyhedron and a cube obtained as the result of the digital curvature flow.

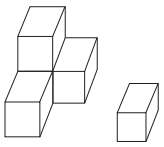

(a) (b)

Figure 5.3: Example of deformation. (a) is transformed to (b). Furthermore, In the next step, $\mathbf{P}$ converges the point $(1,1,1)^\top$

The curvature flow transforms each planar curve segment passing through lattice points on a polyhedral boundary to a straight line segment passing through lattice points on a polyhedral boundary. Furthermore, each closed curve on a plane is transformed to a rectangle. If $\gamma(\boldsymbol{x}) = (+,+,+)$ at each step, the digital curvature flow eliminates 3/4 unit area from the corners. Moreover, positive and negative parts on the boundary move outward and inward, respectively. These considerations conclude the following theorems.

Theorem 20. *For a closed surface, in each step, the digital curvature flow shrinks the boundary on each planar 6 unit area from corners such that* $\gamma(\boldsymbol{x}) = (+,+,+)$.

Theorem 21. *The digital curvature flow preserves the topology if there is no tunnel.*

Theorem 22. *The digital curvature flow transforms a boundary to a cuboid.*

Theorem 23. *The final form of the digital curvature flow is a spatial rectangle.*

Furthermore, setting the surface energy.

$$E = \boldsymbol{k}^\top \boldsymbol{n}, \tag{5.22}$$

we have the following theorem.

Theorem 24. *On a closed two-dimensional manifold* $\partial\mathbf{F}$ *in* $\mathbf{Z}^3$

$$E = \boldsymbol{k}^\top \boldsymbol{n} \geq 8(1+g). \tag{5.23}$$

(*Proof*) From theorems 20, 21, 22 and 23, if $\mathbf{F}$ has no hole, $\mathbf{F}$ is topologically equivalent to a cuboid. Since $E = 8$ for a cuboid, $E \geq 8$ for an object without holes. Furthermore, if an object has g holes, the object is topologically equivalent to a cuboid with g cuboid tunnels. Therefore, for an object with g tunnels, $E \geq 8(1+g)$. □

Moreover, we have the following theorem for E from theorem 20.

Theorem 25. *For the surface evolution of eq. (5.15),* $E = \boldsymbol{k}^\top \boldsymbol{n}$ *satisfies the relation*

$$\frac{\partial E}{\partial t} \leq 0. \tag{5.24}$$

6. Conclusions

We have defined curvature codes on a digital manifold in the three-dimensional digital space $\mathbf{Z}^3$. A point on a 6-connected three-dimensional digital manifold lies on at least two 4-connected planar curves, which lie on a pair of perpendicular digital planes. From this geometrical configuration of orthogonal slices of digital manifolds, the three-dimensional curvature codes were constructed as a combination of three planar curvature codes.

As an extension, we can define the curvature codes of points on an m-dimensional digital manifold in the n-dimensional digital space for $m \leq n-1$. For example, if $m = n-1$, the curvature code on the digital manifold is described in the form $\boldsymbol{\alpha} = (\alpha_1, \alpha_2, \cdots, \alpha_n)$, where $\alpha_i \in \{+1, -1, 0, \emptyset\}$ and the curvature index of this point is

$$f(\alpha_{\pi(1)}, \alpha_{\pi(2)}, \cdots \alpha_{\pi(n)}) = (\sum_{i=1}^{n} s(\alpha_{\pi(i)})) \times (\Pi_{i=1}^{n} |s(\alpha_{\pi(i)})|). \tag{6.1}$$

Theorem 11, which characterizes the topology of closed surfaces in the three-dimensional digital surface, is a digital version of the Gauss-Bonnet theorem. This theorem suggests that using the curvature codes on a higher-dimensional digital manifold, the digital version of the Chern-Gauss-Bonnet theorem can be constructed as

$$\boldsymbol{a}^\top \boldsymbol{n} = 2^n(1-g), \tag{6.2}$$

where $\boldsymbol{a}$ and $\boldsymbol{n}$ are vectors which define the weights for the configurations of points on the surface and the number of configurations on the surface, respectively, and g is the number of the holes of an object. Moreover, the surface energy

$$E = \boldsymbol{k}^\top \boldsymbol{n} = 2^n(1+g), \tag{6.3}$$

where each element of the vector $\boldsymbol{k}$ is the square of the corresponding element of $\boldsymbol{a}$, will satisfy the inequality $\frac{\partial E}{\partial t} \leq 0$.

References

[1] Marshall Bern and David Eppstein. Mesh generation and optimal triangulation. *Computing in Euclidean Geometry, 2nd Edition*, pages 47–123, 1995.

[2] Hanspeter Bieri and Walter Nef. A recursive sweep-plane algorithm, determining all cells of a finite division of R^d. *Computing*, 28:189–198, 1982.

[3] Hanspeter Bieri and Walter Nef. A sweep-plane algorithm for computing the volume of polyhedra represented in Boolean form. *Linear Algebra and Its Applications*, 52/53:69–97, 1983.

[4] Hanspeter Bieri and Walter Nef. Algorithms for the euler characteristic and related additive functionals of digital objects. *CVGIP*, 28:166–175, 1984.

[5] Hanspeter Bieri and Walter Nef. A sweep-plane algorithm for computing the euler-characteristic of polyhedra represented in boolean form. *Computing*, 34:287–304, 1985.

[6] Alexander I. Bobenko and Yuri B. Suris. *Discrete Differential Geometry: Integrable Structure*. American Mathematical Society, 2008.
[7] Alfred M. Bruckstein, Guillermo Shapiro, and Doron Shaked. Evolution of planar polygons. *J. Pattern Recognition and Artificial Intelligence*, 9:991–1014, 1995.
[8] Bastien Chopard and Michel Droz. *Cellular Automata Modeling of Physical Systems*. Cambridge University Press, Cambridge, 1998.
[9] Nira Dyn, David Levinand, and Samuel Rippa. Data dependent triangulations for piecewise linear interpolation. *IMA J. Numerical Analysis*, 10:137–154, 1990.
[10] Gerhard Huisken. Flow by mean curvature of convex surface into sphere. *J. Differential Geometry*, 20:237–266, 1984.
[11] Atsushi Imiya. Geometry of three-dimensional neighbourhood and its applications (in Japanese). *Trans. of Information Processing Society of Japan*, 34:2153–2164, 1993.
[12] Yukiko Kenmochi and Atsushi Imiya. Deformation of discrete object surfaces. *Lecture Notes in Computer Science*, 1296:146–153, 1997.
[13] Ron Kimmel. *Numerical Geometry of Images: Theory, Algorithms, and Applications*. Springer, Heidelberg, 2007.
[14] Reinhard Klette and Azriel Rosenfeld. *Digital Geometry: Geometric Methods for Digital Picture Analysis*. Morgan Kaufmann, 2004.
[15] C.-N Lee, T. Poston, and Azriel Rosenfeld. Holes and genus of 2D and 3D digital images. *CVGIP*, 55:20–47, 1993.
[16] Douglas Lind and Brian Marcus. *An Introduction to Symbolic Dynamics and Coding*. Cambridge University Press, Cambridge, 1995.
[17] Tony Lindeberg. *Scale-Space Theory*. Kluwer Academic Publishers, Dordrecht, 1994.
[18] Tony Lindeberg. Generalized axiomatic scale-space theory. *Advances in Imaging and Electron Physics*, 178:1–96, 2013.
[19] Atsuyuki Okabe, Barry Boots, and Kokichi Sugihara. *Spatial Tessellations: Concepts and Applications of Voronoi Diagrams*. John Wiley& Sons, Chichester, 1992.
[20] Samuel Rippa. Minimal roughness property of the Delaunay triangulation. *Computer Aided Geometric Design*, 7:489–497, 1990.
[21] Tomoya Sakai, Masaki Narita, Takuto Komazaki, Haruhiko Nishiguchi, and Atsushi Imiya. Image hierarchy in gaussian scale space. *Advances in Imaging and Electron Physics*, 165:175–263, 2011.
[22] Guillermo Sapiro. *Geometric Partial Differential Equations and Image Analysis*. Cambridge University Press, Cambridge, 2001.
[23] James A. Sethian. *Level Set Methods: Evolving Interfaces in Geometry Fluid Mechanics, Computer Vision, and Material Science*. Cambridge University Press, Cambridge, 1996.
[24] Junichiro Toriwaki. *Digital Image Processing for Image Understanding, Vols.1 and 2 (in Japanese)*. Syokodo, Tokyo, 1988.
[25] Junichiro Toriwaki, Sigeki Yokoi, T. Yonekura, and T. Fukumura. Topological properties and topological preserving transformation of a three-dimensional binary picture. In *Proc. of the 6th ICPR*, pages 414–419, 1982.
[26] Junichiro Toriwaki and Hiroyuki Yoshida. *Fundamentals of Three-dimensional Digital Image Processing*. Springer, Heidelberg, 2009.
[27] Andrea Toselli and Olof Widlund. *Domain Decomposition Methods - Algorithms and Theory*. Springer, Heidelberg, 2005.
[28] Richard S. Varge. *Matrix Iterative Analysis, 2nd rev. and exp. ed.* Springer, Heidelberg, 2000.
[29] Joachim Weickert. *Anisotropic Diffusion in Image Processing, ECMI Series*. Teubner-Verlag, Stuttgart, 1998.
[30] Stephan Wolfram. *A New Kind of Science*. Wolfram Media, Champaign, 2002.
[31] T. Yonekura, Junichiro Toriwaki, T. Fukumura, and Sigeki Yokoi. On connectivity and the euler number of three-dimensional digitized binary picture. *Trans. of IECE Japan*, E63:815–816, 1980.

Supercomputing Laboratory, Institute of Management and Information Technologies, Chiba University, Yayoi-cho 1-33, Inage-ku, Chiba, 263-8522, Chiba, Japan • imiya@facaulty.chiba-u.jp